

# Supporting Information

## First steps to rationalize host-guest interaction between $\alpha$ -, $\beta$ -and $\gamma$ -cyclodextrin and divalent first row transition and post-transition metals (subgroup VIIIB, VIIIIB and IIB)

Héloïse Dossmann<sup>1</sup>, Lucas Fontaine<sup>2</sup>, Teddy Weisgerber<sup>2</sup>, Véronique Bonnet<sup>2</sup>, Eric Monflier<sup>3</sup>, Anne Ponchel<sup>3</sup>, and Cédric Przybylski<sup>1\*</sup>

<sup>1</sup> Sorbonne Université, CNRS, Institut Parisien de Chimie Moléculaire, IPCM, F-75005 Paris, France.

<sup>2</sup> Université de Picardie Jules Verne, Laboratoire de Glycochimie, des Antimicrobiens et des Agroressources, LG2A, CNRS UMR 7378, 80039 Amiens, France.

<sup>3</sup> Université d'Artois, CNRS, Centrale Lille, ENSCL, Université de Lille, UMR 8181, Unité de Catalyse et de Chimie du Solide (UCCS), F-62300 Lens, France.

\* Email: [cedric.przybylski@sorbonne-universite.fr](mailto:cedric.przybylski@sorbonne-universite.fr)

**Text S1.** Brief report on UV-visible spectroscopy experiences. p.2

**Figure S1.** Example of UV-visible spectrum of ternary complex between p-nitrophenol and  $\beta$ -CD upon some addition of  $\text{Fe}(\text{Cl})_2$  p.2

**Table S1.** Binding energies ( $E_{\text{ass}}$ ) for the three most stable conformers between one transition metal cation and various CDs obtained at the B3LYP/Def2-SV(P) level. p.3

**Figure S2.** Mass spectra of  $\alpha$ -CD with (A)  $\text{FeCl}_2$ , (B)  $\text{CoCl}_2$ , (C)  $\text{NiCl}_2$  and (D)  $\text{CuCl}_2$ . p.4

**Figure S3.** Mass spectra of  $\beta$ -CD with (A)  $\text{FeCl}_2$ , (B)  $\text{CoCl}_2$ , (C)  $\text{NiCl}_2$  and (D)  $\text{CuCl}_2$ . p.5

**Figure S4.** Mass spectra of  $\gamma$ -CD with (A)  $\text{FeCl}_2$ , (B)  $\text{CoCl}_2$ , (C)  $\text{NiCl}_2$  and (D)  $\text{CuCl}_2$ . p.6

**Figure S5** Survival yield curves obtained for doubly charged species of  $\alpha$ -CD (A),  $\beta$ -CD (B), and  $\gamma$ -CD (C) with the various metals upon HCD dissociation mode p.7

**Table S2.** Binding energies ( $E_{\text{ass}}$ ) for the three most stable conformers between one transition metal cation and various CDs obtained at the B3LYP/Def2-SV(P) level. p.8

**Figure S6.** Survival yield curves offset taking into account only loss of 1 glucose unit of  $\beta$ -CD,  $\beta$ -CD and  $\beta$ -CD with the various metals before (A, C and E) and after (B, D and F). p.9

**Text S1.** Brief report on UV-visible spectroscopy experiences.

Stock solution of  $\beta$ -cyclodextrin, *p*-nitrophenol and metal chloride at  $5.10^{-5}$  mol.L<sup>-1</sup> were prepared in ultrapure water. For UV titration, an equimolar mixture of  $\beta$ -cyclodextrin and *p*-nitrophenol both at  $5.10^{-5}$  mol.L<sup>-1</sup> was used with a set of solutions with different metal ion concentrations varying from  $5.10^{-7}$  to  $5.10^{-5}$  mol.L<sup>-1</sup>. All the absorption spectra were recorded in a JASCO spectrophotometer between 200 and 600 nm. Spectrophotometric methods are commonly used for the study of host-guest complexes involving encapsulation of molecules in hydrophobic cavity of CD in solution. Nevertheless, such approach remains arduous or even impossible when CD ligand is a metal which presents no or very low absorbance properties. A frequently adopted methodology to overcome such bottleneck holds in the introduction of UV-visible active molecules which are encapsulated by CD, follows by addition of studied ligands.(Annalakshmi, S.; Pitchumani, K. *Eur. J. Org. Chem.* **2006**, (4), 103.) The increase of the amount of ligand induced a shift in one or more characteristic wavelength of the encapsulated molecules. Even with such alternative, only few studies report its application for CD-metal complexes, using most of time modified CDs and not native ones and leading to sometimes questionable deduced results. To evaluate if such method could be suitable as analytical method to probe CD-metal interactions in solution, we have tested a preformed complex of  $\beta$ -CD and *p*-nitrophenol (pKa 7.14). Solution can change from colorless-light yellow to light/dark yellow portraying the acid-base equilibrium between *p*-nitrophenol ( $\lambda_{\text{max}} = 318$  nm) and *p*-nitrophenolate ( $\lambda_{\text{max}} = 402$  nm). At a given and constant concentration of  $5.10^{-5}$  mol.L<sup>-1</sup> for both  $\beta$ -CD and *p*-nitrophenol, UV-visible spectrum effectively presents two maxima of absorption at the aforementioned wavelengths. Change in spectrum was recorded by varying metal concentration from  $5.10^{-5}$  to  $1.10^{-6}$  mol.L<sup>-1</sup>. Each metal addition yields to an increase of absorbance at 318 nm and a decrease at 402 nm, as well as by an isobestic point at 344 nm only between  $1.10^{-5}$  to  $1.10^{-6}$  mol.L<sup>-1</sup> range (Figure S1). Whatever the metal addition, various perturbing effect was observed onto original equilibrium between *p*-nitrophenol and *p*-nitrophenolate. Nevertheless, it was not possible to exactly delineate the mechanism(s) involved since at least two competitive reactions can be considered: i) formation of a complex between of CD with metals and/or ii) a better complexation of phenolate with metal ions than aliphatic alcohols. Herein, it clearly appears that UV-visible spectroscopy do not constitute a suitable method to probe native CD-metals complexes in only pure water or water/alcohol mixture.

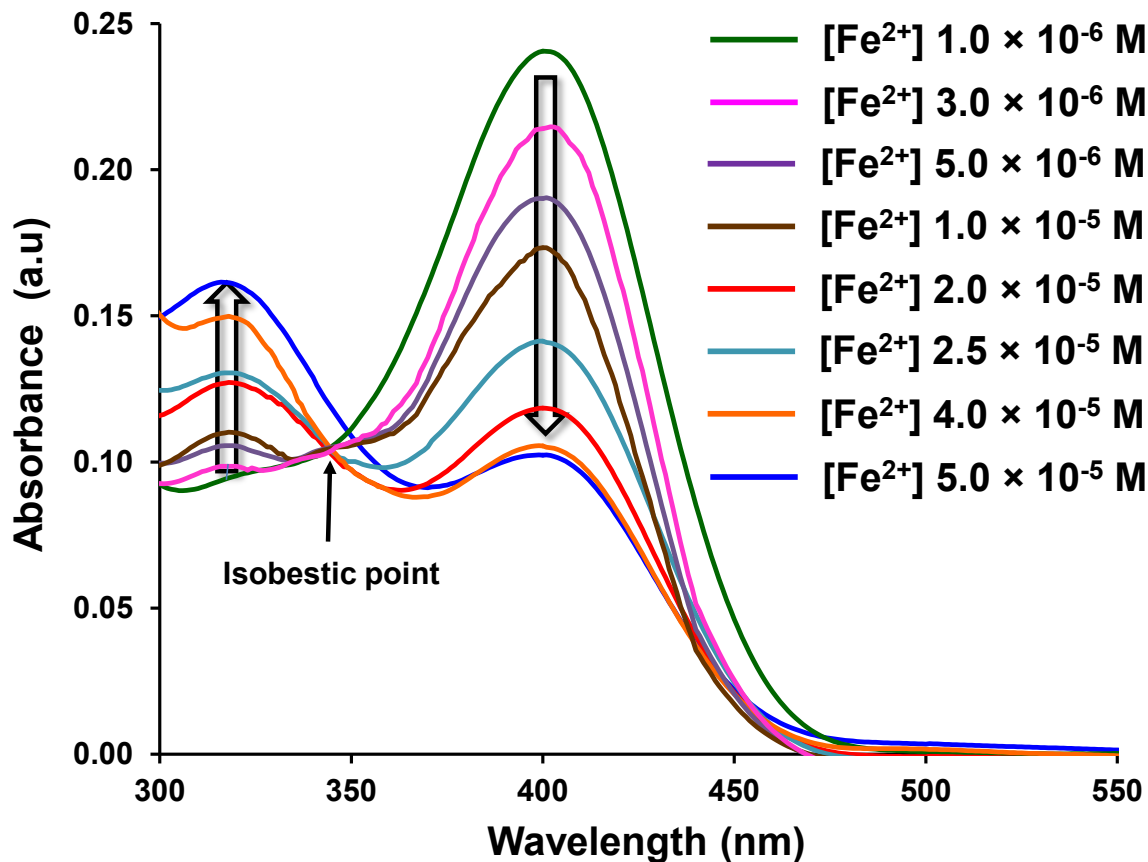


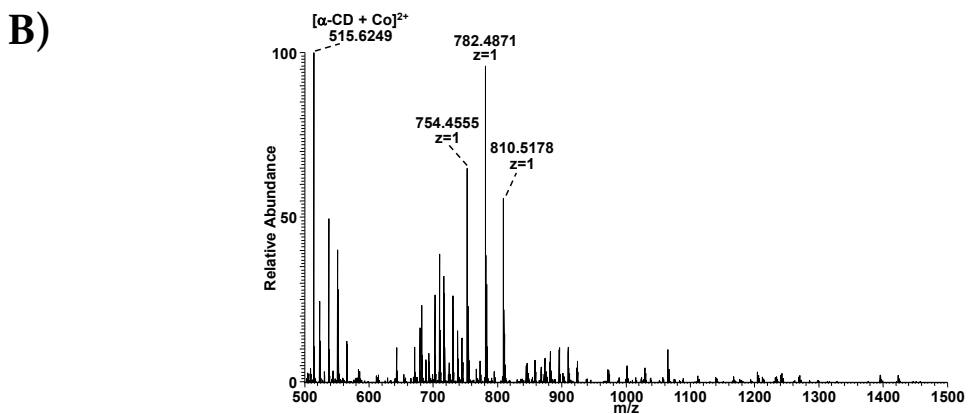
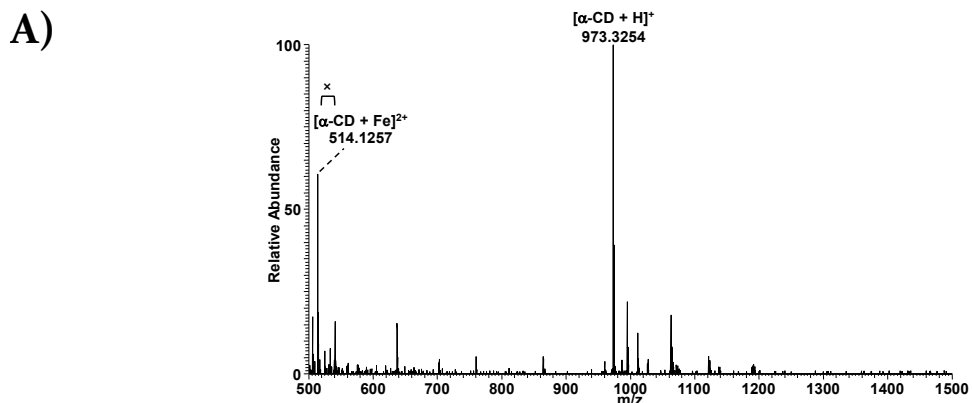
**Figure S1.** Example of UV-visible spectrum of ternary complex between *p*-nitrophenol ( $5 \times 10^{-5} \text{ mol.L}^{-1}$ ) and  $\beta$ -CD ( $5 \times 10^{-5} \text{ mol.L}^{-1}$ ) upon some addition of  $\text{Fe}(\text{Cl})_2$  varying from  $1 \times 10^{-6}$  to  $5 \times 10^{-5} \text{ mol.L}^{-1}$  in water at room temperature.

**Table S1. Binding energies ( $E_{\text{ass}}$ ) for the three most stable conformers between one metal cation and various CDs obtained at the B<sub>3</sub>LYP/Def2-SV(P) level.**

Metal (spin) <sup>a</sup>	$\alpha$ -CD		$\beta$ -CD		$\gamma$ -CD	
	Conformer	$E_{\text{ass}}$ (kcal.mol <sup>-1</sup> )	Conformer	$E_{\text{ass}}$ (kcal.mol <sup>-1</sup> )	Conformer	$E_{\text{ass}}$ (kcal.mol <sup>-1</sup> )
$\text{Mn}^{2+}$ (Q)	ccccw	-329.4	cwcw	-328.3	cccc	-336.5
	cwcw	-322.1	cccc	-317.4	cwcw	-335.4
	cwcc	-321.7	cccw	-309.8	occcc	-319.4
$\text{Fe}^{2+}$ (S)	cwcw	-342.8	cccw	-348.3	cccw	-356.6
	cwcc	-341.3	cwcw	-332.4	cccc	-337.7
	cccw	-338.3	cccc	-327.3	occcc	-342.7
$\text{Co}^{2+}$ (Q)	cwcw	-329.3	cwcw	-333.1	cwcw	-344.5
	cccw	-326.1	cccc	-326.5	cccw	-342.3
	cccc	-322.1	cwcc	-324.2	cccc	-335.0
$\text{Ni}^{2+}$ (S)	cccw	-396.3	cwcw	-397.9	cwcc	-412.9
	cccc	-386.2	cccc	-394.2	cccw	-404.0
	cwcw	-378.4	cccw	-391.6	cccc	-380.4

	CWCW	-355.2	CCCW	-358.4	CWCW	-374.8
<b>Cu<sup>2+</sup> (D)</b>	cccc	-349.3	cwcc	-353.9	cccc	-363.8
	cwcc	-349.2	cccc	-353.0	cwcc	-361.5
<b>Zn<sup>2+</sup> (S)</b>	cwcw	-326.6	cwcw	-340.6	cwcw	-344.6
	cccc	-323.2	cccc	-328.6	cccw	-338.8
	cccw	-321.8	cwcc	-326.2	cccc	-327.6

<sup>a</sup> Most stable spin multiplicity: singlet (S), doublet (D) and quartet (Q).



**C)**

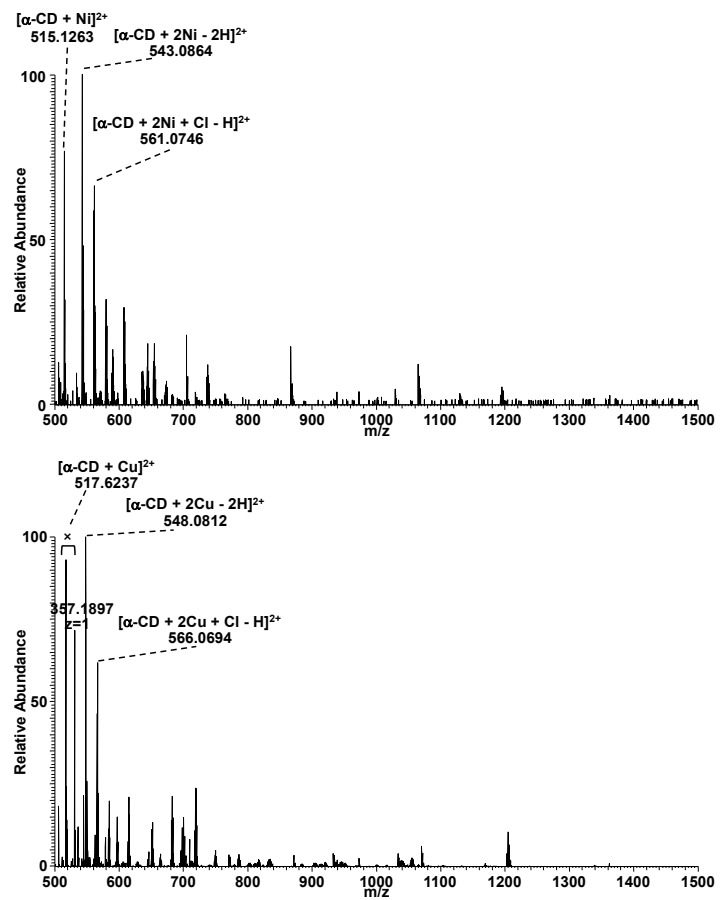


**Figure S2.** Mass spectra of  $\alpha$ -CD with (A)  $\text{FeCl}_2$ , (B)  $\text{CoCl}_2$ , (C)  $\text{NiCl}_2$  and (D)  $\text{CuCl}_2$ . Cyclodextrin and metal chloride were at 10  $\mu\text{M}$  and 100  $\mu\text{M}$ , respectively.

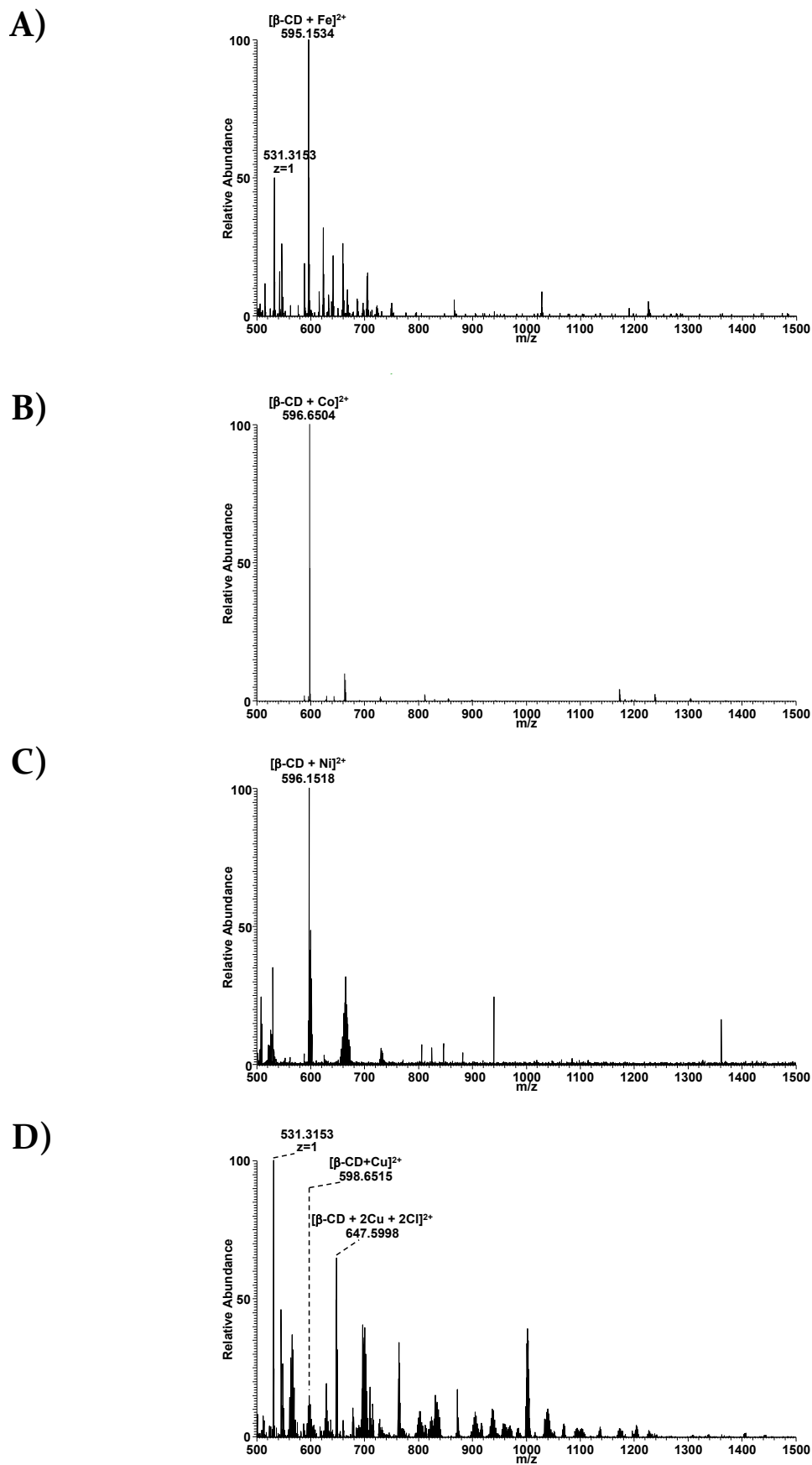


**Figure S3.** Mass spectra of  $\beta$ -CD with (A)  $\text{FeCl}_2$ , (B)  $\text{CoCl}_2$ , (C)  $\text{NiCl}_2$  and (D)  $\text{CuCl}_2$ . Cyclodextrin and metal chloride were at 10  $\mu\text{M}$  and 100  $\mu\text{M}$ , respectively.

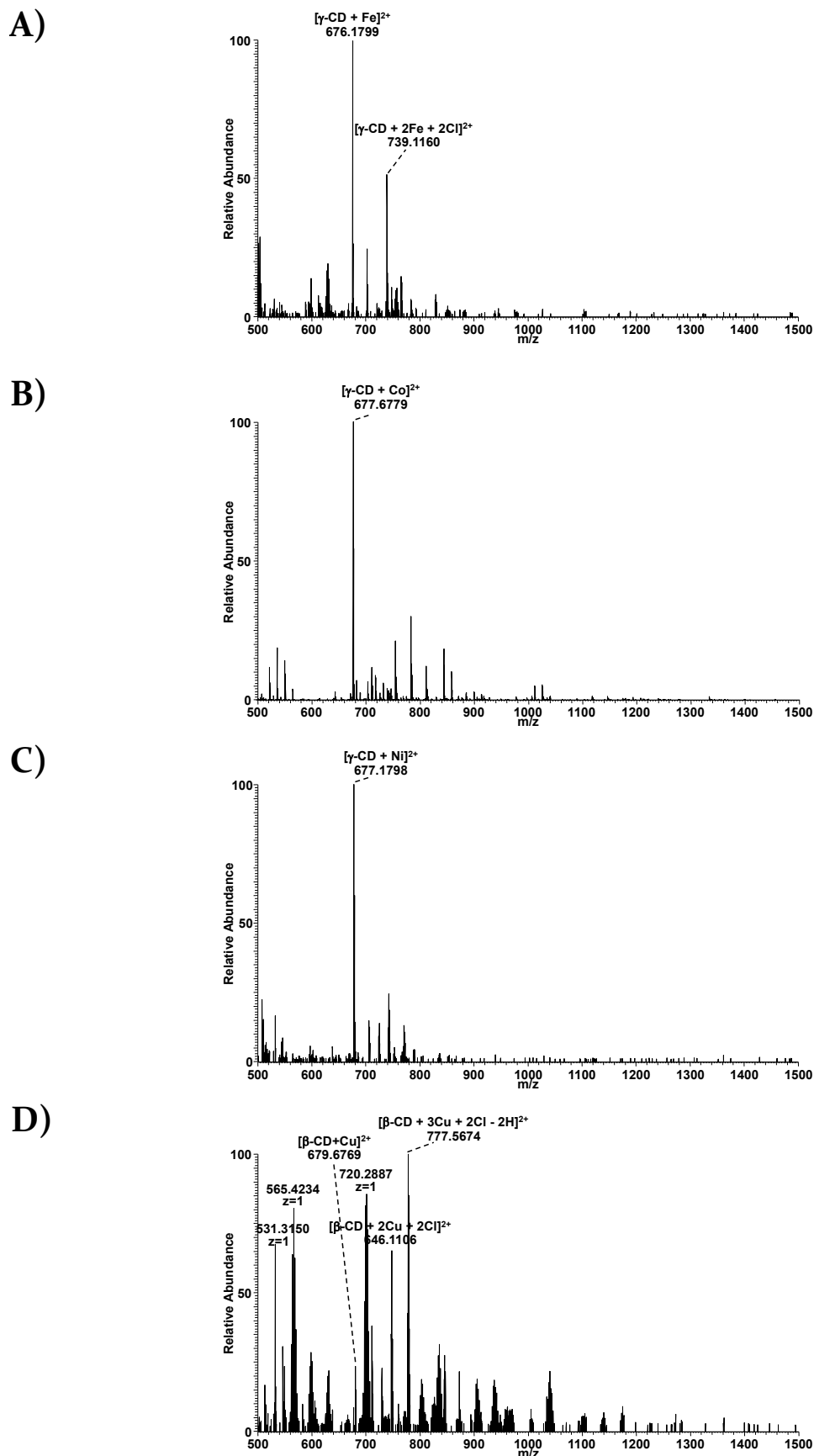


**Figure S4.** Mass spectra of  $\gamma$ -CD with (A)  $\text{FeCl}_2$ , (B)  $\text{CoCl}_2$ , (C)  $\text{NiCl}_2$  and (D)  $\text{CuCl}_2$ . Cyclodextrin and metal chloride were at 10  $\mu\text{M}$  and 100  $\mu\text{M}$ , respectively.

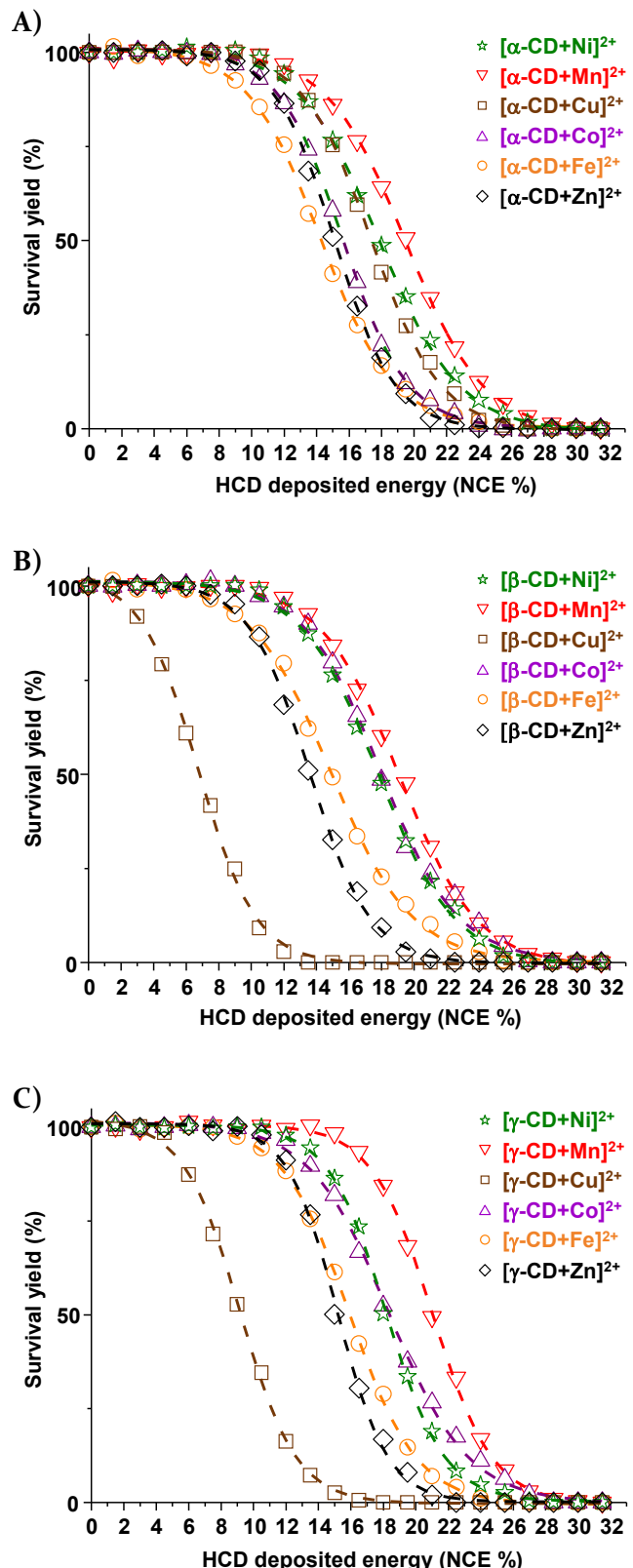


**Figure S5.** Survival yield curves obtained for doubly charged species of  $\alpha$ -CD (A),  $\beta$ -CD (B), and  $\gamma$ -CD (C) with the various metals upon HCD dissociation mode.

**Table S2. Recapitulative of characteristic CE<sub>50</sub> values obtained for the CD- metals complexes. Standard deviation obtained for 3 m/z determinations was 0.1%.**

Metal	m/z ([CD+Metal] <sup>2+</sup> )		Mass accuracy (ppm)	HCD CE <sub>50</sub>	
	Exp.	Theo.		%	eV
$\alpha$ -CD	Mn <sup>2+</sup>	513.6277	513.6269	1.6	19.1 19
	Fe <sup>2+</sup>	514.1257	514.1254	0.6	15.4 15
	Co <sup>2+</sup>	515.6249	515.6245	0.8	16.7 17
	Ni <sup>2+</sup>	515.1263	515.1256	1.4	17.9 18
	Cu <sup>2+</sup>	517.6237	517.6227	1.9	17.6 18
	Zn <sup>2+</sup>	518.1235	518.1225	1.9	16.1 16
$\beta$ -CD	Mn <sup>2+</sup>	594.6544	594.6534	1.7	19.1 22
	Fe <sup>2+</sup>	595.1534	595.1518	2.7	14.9 17
	Co <sup>2+</sup>	596.6504	596.6509	0.8	17.9 19
	Ni <sup>2+</sup>	596.1518	596.1520	0.3	17.8 21
	Cu <sup>2+</sup>	598.6506	598.6491	2.5	6.7 8
	Zn <sup>2+</sup>	599.1497	599.1489	1.3	13.6 16
$\gamma$ -CD	Mn <sup>2+</sup>	675.6807	675.6798	1.3	21.0 28
	Fe <sup>2+</sup>	676.1799	676.1782	2.5	15.9 20
	Co <sup>2+</sup>	677.6779	677.6773	0.9	18.3 21
	Ni <sup>2+</sup>	677.1798	677.1784	2.1	18.2 24
	Cu <sup>2+</sup>	679.6769	679.6755	2.1	9.2 12
	Zn <sup>2+</sup>	680.1768	680.1753	2.2	15.2 16

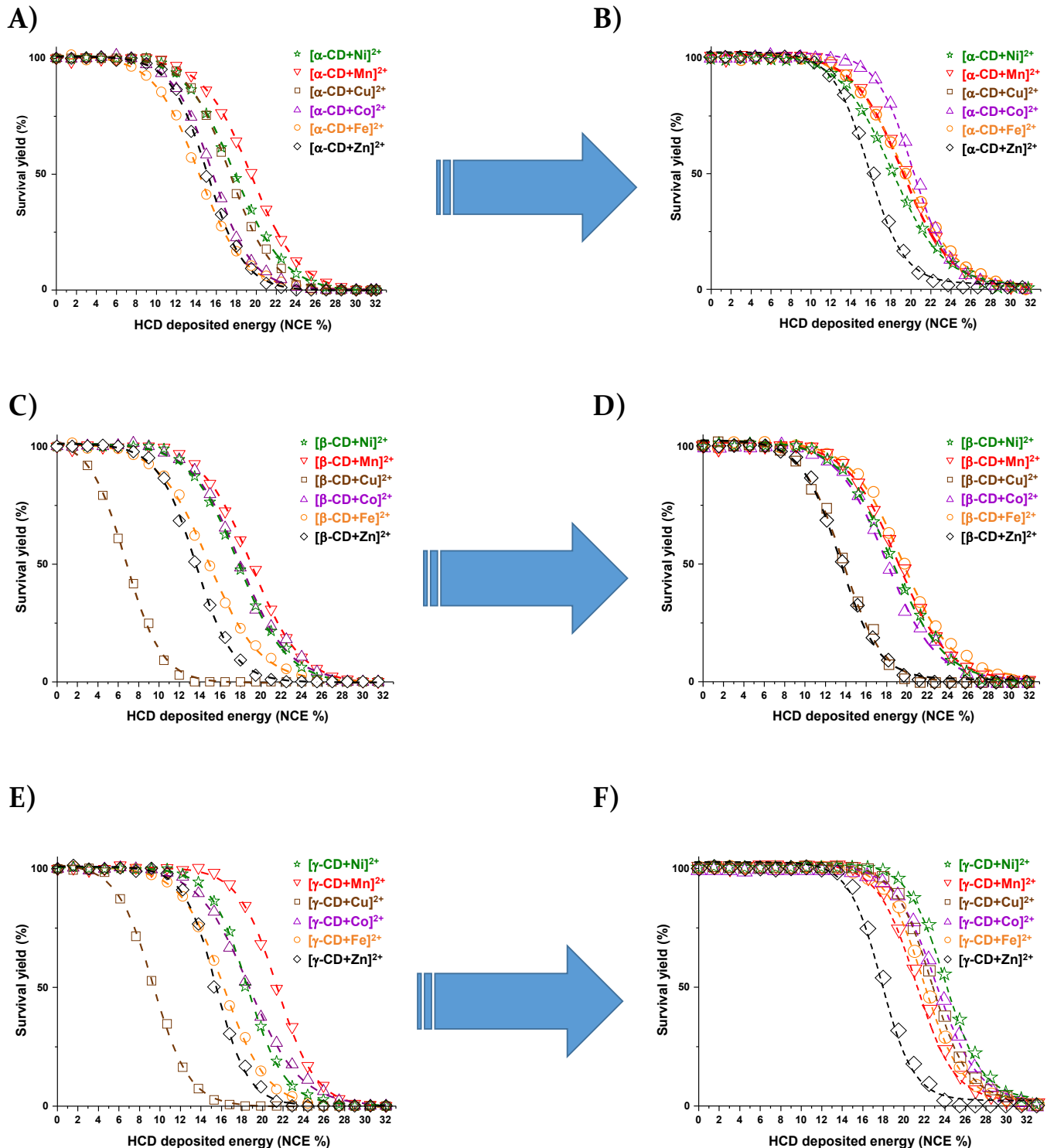


**Figure S6.** Survival yield curves of  $\alpha$ -CD,  $\beta$ -CD and  $\gamma$ -CD with the various metals before (A, C and E) and after (B, D and F) offset taking into account only loss of 1 glucose unit.

